International Journal of Automotive Technology, Vol. 18, No. 2, pp. 271–277 (2017)
DOI 10.1007/s12239–017–0027–3

pISSN 1229–9138/ eISSN 1976–3832

COORDINATED CONTROL OF ESC AND AFS WITH ADAPTIVE ALGORITHMS

S. YIM*

Department of Mechanical and Automotive Engineering, Seoul National University of Science and Technology, Seoul 01811, Korea

(Received 20 October 2015; Revised 20 June 2016; Accepted 5 July 2016)

ABSTRACT–This paper presents a coordinated control of electronic stability control (ESC) and active front steering (AFS) with adaptive algorithms for yaw moment distribution in integrated chassis control (ICC). In order to distribute a control yaw moment into control tire forcres of ESC and AFS, and to coordinate the relative usage of ESC to AFS, a LMS/Newton algorithm (LMSN) is adopted. To make the control tire forces zero in applying LMS and LMSN, the zero-attracting mechanism is adopted. Simulations on vehicle simulation software, CarSim®, show that the proposed algorithm is effective for yaw moment distribution in integrated chassis control.

KEY WORDS : Integrated chassis control, Electronic stability control, Active front steering, Adaptive algorithms, Zero-attracting mechanism

NOMENCLATURE

C_f, C_r : cornering stiffness of front/rear tires (N/rad)
e_k : adaptation error at time instant k
F_x, F_y, F_z : longitudinal/lateral/vertical tire forces (N)
F_{yf}, F_{yr} : lateral tire force of front/rear wheels (N)
G : effectiveness matrix
I : identity matrix
I_z : yaw moment of inertial (kg×m^2)
J_1, J_2 : objective functions of adaptive algorithms
K_γ : steady-state yaw rate gain (1/s)
K : gain in sliding mode control
K_B : pressure-force constant (N×m/MPa)
l_f, l_r : distance from C.G. to front/rear axles (m)
m : vehicle total mass (kg)
P_B : brake pressure (MPa)
H : weighting matrix in LLMS
Q, **R** : auto-correlation and cross-correlation matrices in LMSN and ZA-LMSN
r_w : radius of a wheel (m)
s : sliding surface
$2t_f$, $2t_r$: front/rear track widths (m)
V : vehicle velocity (m/s)
v_x, v_y : longitudinal/lateral velocities of a vehicle (m/s)
w : vector of the control tire forces
β : side-slip angle (rad)
δ_f : steering angle of front wheels (rad)
$\Delta\delta_f$: corrective steering angle by AFS (rad)
ΔF_x : longitudinal tire force by ESC (N)
ΔF_{yf} : lateral tire force by AFS (N)
ΔM_B : control yaw moment
γ, γ_d : real and reference yaw rates (rad/s)
η : tuning parameter on side-slip angle
ε : convergence rate of LMS and its variants
ρ : tuning parameter on zero-attracting term
μ : tire-road friction coefficient

*Corresponding author. e-mail: acebtif@seoultech.ac.kr

1. INTRODUCTION

Vehicle stability control is to generate a control yaw moment, which is needed to stabilize a vehicle under critical situations. There are several objectives in vehicle stability control. The most representative objective is yaw rate tracking or the maneuverability, which makes a vehicle follow the driver's intention (Rajamani, 2006). Another objective is the lateral stability, which maintains the side-slip angle of a vehicle as small as possible (Wong, 2001). When designing a vehicle stability controller, the control yaw moment should be computed in order that these objectives are satisfied.

The control yaw moment should be generated by an actuator in a real vehicle. This is called yaw moment distribution. Several actuators are used for yaw moment distribution. Typical actuator is an electronic stability control (ESC), which uses brake pressures. Besides ESC, active front steering (AFS) or torque vectoring device (TVD) is used for it. These actuators have its own advantages and disadvantages for yaw moment distribution. The advantage of ESC is to reduce the vehicle speed with braking. The reduction of a vehicle speed has a large effect

on safety of a vehicle. However, ESC causes discomfort, which is generated by the longitudinal acceleration and the resulting pitch angle. On the other hand, the advantage of AFS is to generate the control yaw moment without braking. As a result, the smaller extent of the vehicle speed is reduced than ESC. However, high vehicle speed can deteriorates the lateral stability because it generates a large side-slip angle (Cho *et al*., 2008; Yim, 2015, 2016). Generally, it is more effective to use multiple actuators than a single one in yaw moment distribution. When multiple actuators are used for yaw moment distribution, it is called integrated chassis control (ICC) or unified chassis control (UCC) (Cho *et al*., 2008). In this paper, ESC and AFS are used for yaw moment distribution.

For yaw moment distribution in ICC, several approaches have been proposed up to date. The most of these researches have formulated the yaw moment distribution as an optimization problem, and to apply several algorithms to solve it such as a weighted pseudo-inverse based control allocation (WPCA) (Wang and Longoria, 2006; Yim *et al*., 2012), a fixed-point control allocation (Wang *et al*., 2007), an equality-constrained quadratic program (ECQP) (Mokhiamar and Abe, 2004), a quadratically-constrained quadratic program (QCQP) (Schofield, 2006) and etc. Because the most of the optimization problems are non-linear and non-convex, a time-consuming optimization procedure was needed to solve the problem.

Among these, WPCA and ECQP can solve the problem in real time because only the algebraic matrix computation is needed (Wang and Longoria, 2006; Yim *et al*., 2012). However, these methods require numerical computation of matrix inverse, which can cause a numerical instability. Moreover, WPCA require the estimation or measurement of the vertical tire forces and the tire-road friction coefficient. To overcome the drawbacks, it is necessary to apply a method which is fast and easy to implement without extra measurement or estimation. Besides faster and simpler implementation, it is required for adaptive algorithms to coordinate the relative magnitude of the tire force generated by AFS to ESC. For this purpose, adaptive algorithms such as a least-mean-square (LMS) and a leaky LMS (LLMS) were applied to yaw moment distribution (Yim, 2016). WPCA was used as a reference for comparison. In that work, the control tire forces of LMS do not converged to zero as the control yaw moment becomes zero. In LLMS, an extra term was introduced to coordinate ESC and AFS. The extra term in LLMS can deteriorate the yaw moment distribution performance.

To coordinate ESC and AFS, a variant of LMS/Newton (LMSN) algorihtm is adopted in this paper. LMSN does not introduce an extra term, which was used in LLMS. So, LMSN does not deteriorate the performance of yaw moment distribution. The drawback of LMS and LMSN is that it cannot guarantee to make the weights of LMS and LMSN become zero. To overcome the drawback, a zero-forcing or zero-attracting mechanism is adopted to LMS and LMSN (Chen *et al*., 2009; Shi and Shi, 2010). The adaptive algorithms for yaw moment distribution are compared through simulations on a vehicle simulation package, CarSim (Mechanical Simulation Corporation, 2001).

This paper is organized as follows: In Section 2, ICC is designed. The control yaw moment is computed with a sliding mode control theory. Adaptive algorithms for yaw moment distribution are introduced. In Section 3, simulation was conducted on CarSim in order to check the performance of the adaptive algorithms for yaw moment distribution. Section 4 concludes this paper.

2. DESIGN OF INTEGRATED CHASSIS CONTROL

In this section, the integrated chassis control is designed. ICC has two-level control structure: upper- and lower-level controllers. In the upper-level controller, the control yaw moment is computed with controller design methodolody. In the lower-level controller, the control yaw moment is distributed into tire forces generated by ESC and AFS. For yaw moment distribution, adaptive algorithms are adopted.

2.1. Computation of a Control Yaw Moment in the Upper-level Controller

In this subsection, the control yaw moment is computed with a direct yaw moment control (DYC). Figure 1 shows the 2-DOF bicycle model, which is used for DYC. The bicycle model describes the yaw and the lateral motions of a vehicle under the assumption that the longitudinal velocity v_x is constant (Rajamani, 2006). The state variables in the bicycle model are the yaw rate and the side-slip angle. If a relevant lateral tire force model is adopted, the bicycle model becomes suitable to describe the lateral and yaw motions of a real vehicle. In Figure 1, the control input is the control yaw moment, ΔM_B.

The equations of motion for the 2-DOF bicycle model are obtained as follows:

$$\begin{aligned} mv_x(\dot{\beta}+\gamma) &= F_{yf}\cos\delta_f + F_{yr}, \\ I_z\dot{\gamma} &= l_f F_{yf}\cos\delta_f - l_r F_{yr} + \Delta M_B. \end{aligned} \tag{1}$$

Under the assumption that the lateral tire force is linear, the reference yaw rate generated by driver's steering input, δ_f, is given as the algebraic formula in (2) (Rajamani, 2006). In (2), K_γ is a steady-state yaw rate gain, which is a

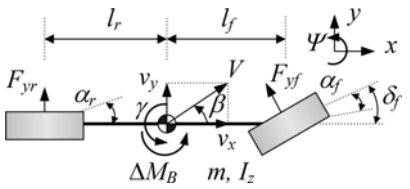

Figure 1. 2-DOF bicycle model.

function of the cornering stiffness, vehicle mass, and longitudinal speed.

$$\gamma_{\mathrm{d}} = \frac{K_{\gamma}}{\tau s + 1} \cdot \delta_{\mathrm{f}} \tag{2}$$

To design a controller, a sliding mode control is adopted. In order to satisfy the maneuverability and the lateral stability, the sliding surface is defined as (3). In (3), η is the parameter used to tune the trade-off between the yaw rate error and the side-slip angle. In order to make the sliding surface zero, the condition (4) should be satisfied (Uematsu and Gerdes, 2002).

$$s = (\gamma - \gamma_{\mathrm{d}}) + \eta \cdot \beta \tag{3}$$

$$\dot{s} = -Ks \quad (K > 0) \tag{4}$$

By differentiating (3) and combining it with (4) and (1), the control yaw moment ΔM_{B} needed to make the sliding surface be zero is obtained as (5).

$$\begin{aligned} \Delta M_{\mathrm{B}} = I_{\mathrm{z}} \cdot \dot{\gamma}_{\mathrm{d}} + I_{\mathrm{z}} \cdot \eta \cdot \left(\frac{F_{\mathrm{yf}} \cos\delta_{\mathrm{f}} + F_{\mathrm{yr}}}{m v_{\mathrm{x}}} - \gamma \right) \\ - l_{\mathrm{f}} F_{\mathrm{yf}} \delta_{\mathrm{f}} + l_{\mathrm{r}} F_{\mathrm{yr}} - I_{\mathrm{z}} \cdot K \cdot (\gamma - \gamma_{\mathrm{d}} + \eta \cdot \beta) \end{aligned} \tag{5}$$

2.2. Yaw Moment Distribution in the Lower-level Controller

Once the control yaw moment ΔM_{B} is computed from the upper-level controller, it should be distributed into the tire forces generated by actuators, ESC and AFS. Figure 2 shows the geometric relationship between the control tire forces and the control yaw moment (Yim, 2015). In Figure 2, ΔF_{x1}, ΔF_{x2}, ΔF_{x3} and ΔF_{x4} are the longitudinal braking forces, which are converted into the braking force of ESC. ΔF_{yf} is the lateral tire force which is converted into the corrective steering angle of AFS. These control tire forces should be determined to generate the control yaw moment ΔM_{B}. This is called yaw moment distribution.

If the control yaw moment is positive, the control tire forces needed to generate the control yaw moment are ΔF_{yf}, ΔF_{x1} and ΔF_{x3}. From Figure 2 (a), the geometric relationship between the control tire forces and the control yaw moment is given in (6). This relationship should always be satisfied

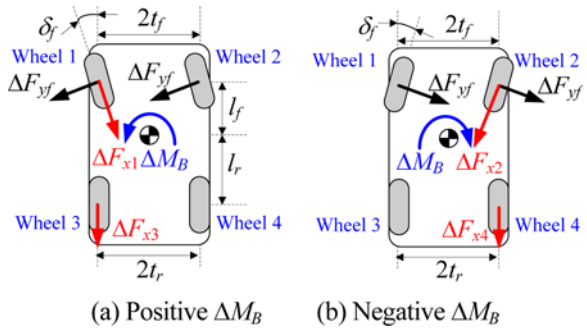

Figure 2. Geometric relationship between the control tire forces and the control yaw moment.

for yaw moment distribution.

$$\underbrace{\begin{bmatrix} -2l_{\mathrm{f}}\cos\delta_{\mathrm{f}} & -t_{\mathrm{f}}\cos\delta_{\mathrm{f}} + l_{\mathrm{f}}\sin\delta_{\mathrm{f}} & -t_{\mathrm{r}} \end{bmatrix}}_{\mathbf{G}} \underbrace{\begin{bmatrix} \Delta F_{\mathrm{yf}} \\ \Delta F_{\mathrm{x1}} \\ \Delta F_{\mathrm{x3}} \end{bmatrix}}_{\mathbf{w}} = \Delta M_{\mathrm{B}} \tag{6}$$

In the previous work, a weighted pseudo-inverse based control allocation (WPCA) was used for yaw moment distribution (Wang and Longoria, 2006; Yim *et al*., 2012). WPCA uses a quadratic objective function, which tries to minimize the control tire forces. With WPCA, the optimum tire force is algebraically calculated. In the objective function of WPCA, the vertical tire forces and the tire-road friction should be estimated because these values cannot be measured or a sensor is too expensive. Although the computation of the optimum solution in WPCA is simple, it requires the matrix inversion, which can generate a numerical instability. So, it is necessary to apply simpler and faster algorithm to yaw moment distribution. This algorithm should be run without numerical instability and require the smaller amount of computation. Typical algorithm for this purpose is least mean square (LMS).

2.3. Adaptive Algorithms for Yaw Moment Distribution

LMS is quite simple enough to be easily implemented. Moreover, it does not require the matrix inversion. From the geometric relationship (6), the adaptation error for yaw moment distribution is defined as (7). Hereafter, k is the time instant. The objective of LMS is to minimize the squared error, as given in (8). The steepest descent update of $\mathbf{w}_{\mathrm{k}}$ is given in (9). With the error and the objective function J_1, the adaptation law of LMS is obtained as (10).

$$e_{\mathrm{k}} = \Delta M_{\mathrm{B,k}} - \mathbf{G}_{\mathrm{k}} \mathbf{w}_{\mathrm{k}} \tag{7}$$

$$J_1 = e_{\mathrm{k}}^2 \tag{8}$$

$$\mathbf{w}_{\mathrm{k+1}} = \mathbf{w}_{\mathrm{k}} - \varepsilon \nabla_{\mathbf{w}} J_1 \tag{9}$$

$$\mathbf{w}_{\mathrm{k+1}} = \mathbf{w}_{\mathrm{k}} + 2\varepsilon e_{\mathrm{k}} \mathbf{G}_{\mathrm{k}}^{\mathrm{T}} \tag{10}$$

LMS in (10) cannot guarantee that the resulting control tire forces become zero if the control yaw moment is zero. To cope with the problem, a zero-forcing or zero-attracting mechanism is adopted (Chen *et al*., 2009; Shi and Shi, 2010). In LMS, the objective function J_1 is modified as J_2, which includes the l_1-norm of $\mathbf{w}_{\mathrm{k}}$ as given in (11). In (11), ρ is the parameter used to tune the relative magnitude of the tire forces to the squared error. The second term of the right-hand side in (11) is called a zero-forcing or zero-attracting term. By adding it to the objective function, $\mathbf{w}_{\mathrm{k}}$ is forced to be zero. By applying (9), the adaptation law for minimizing the objective function J_2 is obtained as (12). This is called zero-attracting LMS or ZA-LMS.

$$J_2 = e_{\mathrm{k}}^2 + \rho \left\| \mathbf{w}_{\mathrm{k}} \right\|_1 \tag{11}$$

$$\mathbf{w}_{\mathrm{k+1}} = \mathbf{w}_{\mathrm{k}} + 2\varepsilon e_{\mathrm{k}} \mathbf{G}_{\mathrm{k}}^{\mathrm{T}} - 2\varepsilon\rho \cdot \mathrm{sgn}(\mathbf{w}_{\mathrm{k}}) \tag{12}$$

LMS has no ability to coordinate the relative magnitude of one element to another in $\mathbf{w}_k$. In other words, it cannot coordinate the relative magnitude of the control tire forces of ESC to AFS in yaw moment distribution. In the previous work, a leaky LMS (LLMS) was adopted to coordinate ESC and AFS (Yim, 2016). In LLMS, the quadratic penalty term $\mathbf{w}^T_k\mathbf{H}\mathbf{w}_k$ was introduced to J_1, as give in (13). The adaptation law of LLMS is given in (14). In (13), **H** is the diagonal matrix, whose the element is the penalty term on the corresponding tire force. If a particular element in **H** increases, then the corresponding tire force decreases. This is equivalent to the variable weights of WPCA (Yim *et al*., 2012). If a particular element in **H** is set to a large value, it makes the convergence of LLMS slower than LMS. As a result, the yaw moment distribution performance was deteriorated by LLMS.

$$J_3 = e_k^2 + \mathbf{w}_k^T\mathbf{H}\mathbf{w}_k \tag{13}$$

$$\mathbf{w}_{k+1} = \mathbf{w}_k + 2\varepsilon e_k\mathbf{G}_k^T - 2\varepsilon\mathbf{H}\mathbf{w}_k \tag{14}$$

To coordinate ESC and AFS in yaw moment distribution without an extra term, a LMS/Newton (LMSN) algorithm is adopted in this paper. Instead of using the update Equation (9), the new one in (15) is used. In (15), **Q** is defined as the auto-correlation matrix, i.e., $\mathbf{w}_k\mathbf{w}^T_k$, which is used to change the steepest search direction to Newton one (Widrow and Sterns, 1985; Diniz, 2008). With the new update Equation (15), the objective function J_1 can be arranged into the new one J_3, as given in (16). In (16), $\mathbf{w}_{opt}$ is the optimum weight, i.e., $\mathbf{w}_{opt} = \mathbf{QR}$, where **Q** and **R** are the auto-correlation matrix of $\mathbf{w}_k$ and the cross-correlation matrix of $\mathbf{w}_k$ and $\Delta M_{B,k}$, respectively (Haykin and Widrow, 2003). In this paper, **Q** is used for another purpose. In the original LMSN, **Q** is updated at each time step in order to estimate the true auto-correlation matrix. On the other hand, **Q** is set to a constant matrix in this paper.

In this paper, **Q** is a diagonal matrix whose the element is used to select which a particular control tire force is generated. If a particular element in $\mathbf{Q}^{-1}$ increases, then the corresponding tire force does. As shown in (6), the first element in $\mathbf{Q}^{-1}$ corresponds to the lateral tire forces generated by AFS. the second and third elements in $\mathbf{Q}^{-1}$ correspond to the front and rear braking forces generated by ESC, respectively. For example, the first element in $\mathbf{Q}^{-1}$ is set to a very large value, then ΔF_{yf} of AFS increases. On the contrary, ΔF_{x1} and ΔF_{x3} of ESC decrease to zero. This is exactly the same as the matrix **H** in LLMS, as shown in (16). In other words, the matrix $\mathbf{Q}^{-1}$ in LMSN is identical to **H** in LLMS. With this manner, the relative magnitude of ΔF_{yf} to ΔF_{x1} and ΔF_{x3} can be set. With the new update equation of (15), the adaptation law of LMSN is obtained as (17).

$$\mathbf{w}_{k+1} = \mathbf{w}_k - \varepsilon\mathbf{Q}^{-1}\nabla_{\mathbf{w}}J_1 \tag{15}$$

$$J_3 = J_1 + (\mathbf{w}_k - \mathbf{w}_{opt})^T\mathbf{Q}(\mathbf{w}_k - \mathbf{w}_{opt}) \tag{16}$$

$$\mathbf{w}_{k+1} = \mathbf{w}_k + 2\varepsilon e_k\mathbf{Q}^{-1}\mathbf{G}_k^T \tag{17}$$

The zero-attracting term can be easily applied to LMSN, as given in (11). The adaptation law with the new update Equation (15) for minimizing the objective function J_3 is obtained as (18). This is called zero-attracting LMSN or ZA-LMSN.

$$\mathbf{w}_{k+1} = \mathbf{w}_k + 2\varepsilon e_k\mathbf{Q}^{-1}\mathbf{G}_k^T - 2\varepsilon\rho\cdot\mathrm{sgn}(\mathbf{w}_k) \tag{18}$$

After obtaining the control tire forces $\mathbf{w}_k$ from the adaptive algorithms, each tire force in $\mathbf{w}_k$ is converted into the braking pressure P_B of ESC and the corrective steering angle $\Delta\delta_f$ of AFS, as given in (19). The identical procedure can be applied in order to obtain the tire forces ΔF_{yf}, ΔF_{x2} and ΔF_{x4} when the control yaw moment is negative, as shown in Figure 2 (b).

$$\begin{aligned} P_{Bi} &= \frac{r_w}{K_B}\Delta F_{xi} \quad (i = 1,\ 2,\ 3,\ 4) \\ \Delta\delta_f &= \frac{\Delta F_{yfc}}{C_f} \end{aligned} \tag{19}$$

3. SIMULATION

Simulation was conducted to check the performance of the adaptive algorithms for yaw moment distribution. Simulation was performed on a vehicle simulation package, CarSim, in connection with MATLAB Simulink.

The vehicle model used in simulation is a small-sized SUV provided in CarSim. Table 1 shows the parameters of the model. The initial speed of vehicle and the tire-road friction coefficient were set to 80 km/h and 0.6, respectively. The actuators for the brake of ESC and steering of AFS were modeled as the first-order systems with the time constants of 0.12 and 0.02, respectively.

The steering input was obtained as a closed-loop steering on a moose test track (Ungoren and Peng, 2004). The driver model used in the simulations was McAdam's one, provided in CarSim (MacAdam, 1981). The preview interval of this driver model was set to 0.75 sec, which means an inexperienced driver.

The first simulation was conducted in order to compare the performance of WPCA, LMS, ZA-LMS and ZA-LMSN. The convergence rates of adaptive algorithms were

Table 1. Parameters of a small-size SUV in CarSim.

m	1146.0 kg	I_z	1302.1 kg·m^2
C_f	39,401 N/rad	C_r	64,119 N/rad
l_f	0.880 m	l_r	1.320 m
$2t_f$	1.465 m	$2t_r$	1.470 m
$K_{B,\,front}$	150 N/MPa	$K_{B,\,rear}$	70 N/Mpa
r_w	0.334 m		

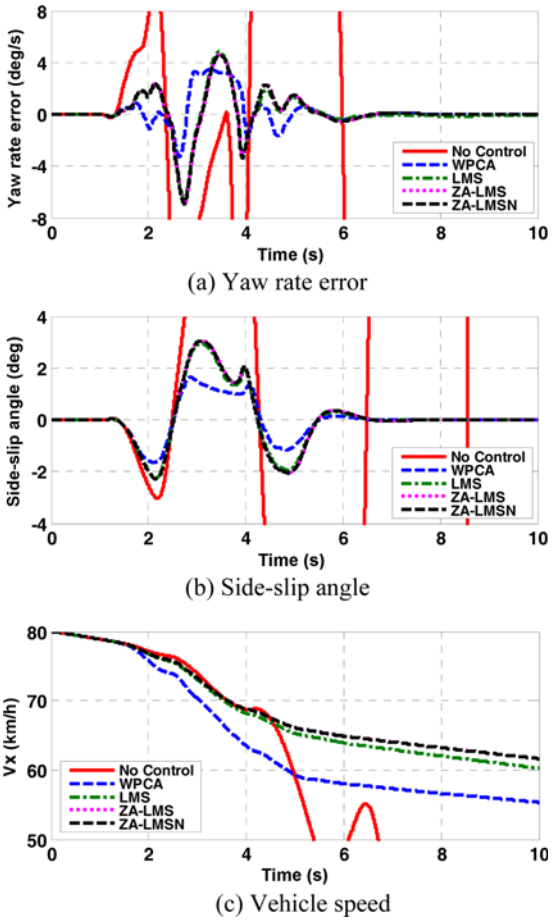

Figure 3. Simulation results for each adaptive algorithm.

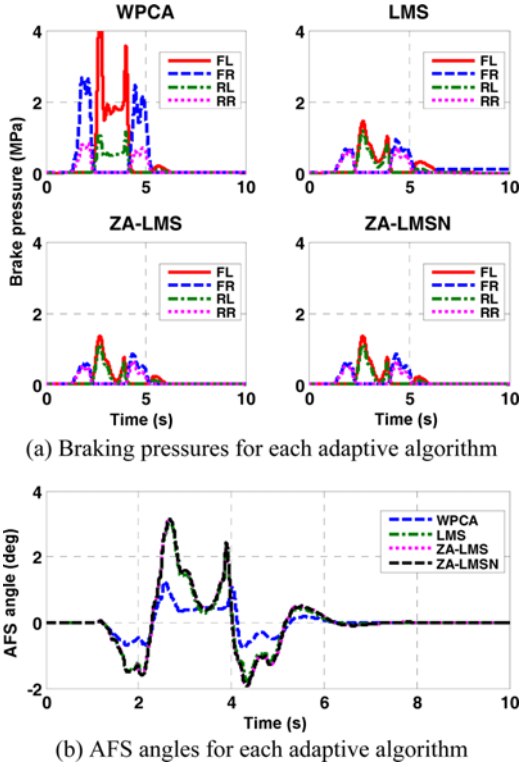

Figure 4. Control inputs for each adaptive algorithm.

set to 0.05. $\mathbf{Q}^{-1}$ in ZA-LMSN was set to $0.1\mathbf{I}$. If $\mathbf{Q}^{-1}$ is smaller than $0.1\mathbf{I}$, it has little effects on the relative magnitudes of control tire forces. In other words, ZA-LMSN becomes ZA-LMS.

Figures 3 and 4 show the simulation results and control inputs for each yaw moment distribution algorithms, respectively. In Figure 4, the legends FL, FR, RL and RR represents the front left, front right, rear left and rear right wheels, respectively.

As shown in Figures 3 and 4, the uncontrolled vehicle lost its stability due to the excessive steering on a low-friction road. On the contrary, the controlled vehicles maintained its stability. The results imply that ICC is effective for vehicle stability. Figures 3 and 4 show that all the adaptive algorithms gave the nearly identical results. This is caused by the fact that ZA-LMS and ZA-LMSN are basically LMS. Moreover, the adaptive algorithms gave identical weights on the braking of ESC and steering of AFS. ZA-LMSN with the matrix $\mathbf{Q}^{-1}$ of $0.1\mathbf{I}$ acts like ZA-LMS because $\mathbf{Q}^{-1}$ is small. As shown in Figure 4 (a), the brake pressures of LMS did not converge to zero. It means that LMS cannot be applied for yaw moment distribution purpose. On the contrary, the brake pressures of adaptive algorithms with zero-attracting mechanism, i.e., ZA-LMS and ZA-LMSN, became zero. This fact caused the slight different results among the adaptive algorithms. From the simulation results, it can be known that LMS and LMSN with the zero-attracting mechanism are effective for yaw moment distribution. WPCA gives the smallest side-slip angle and vehicle speed because the largest braking pressures and the smallest AFS angle were applied, as shown in Figure 4. On the other hand, three adaptive algorithms gave the larger side-slip angles and vehicle speeds because the smaller braking pressures were applied than WPCA.

To check the effect of the relative variation of the one element to others in $\mathbf{Q}$ for ZA-LMSN, the second simulation was conducted on the identical condition to the first one. The convergence rate of ZA-LMSN was set to 0.05. Three cases of elements in $\mathbf{Q}^{-1}$ were considered. Case 1, 2 and 3 correspond to the set of elements (10,0.1,0.1), (0.1,0.1,0.1), and (0.1,10,10) in $\mathbf{Q}^{-1}$, respectively. Case 1 highly penalized the braking forces, ΔF_{x1} and ΔF_{x3} generated by ESC. So, AFS will be used for yaw moment distribution without the aid of ESC. On the other hand, Case 3 highly penalized the lateral tire force, ΔF_{yf} generated by AFS. So, ESC will be used for yaw moment distribution without the aid of AFS. From this fact, it was expected that Case 1 gives the largest side-slip angle and vehicle speed and the smallest braking pressures.

Figures 5 and 6 show the simulation results and control

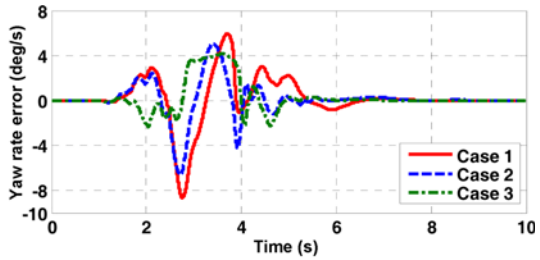

(a) Yaw rate error

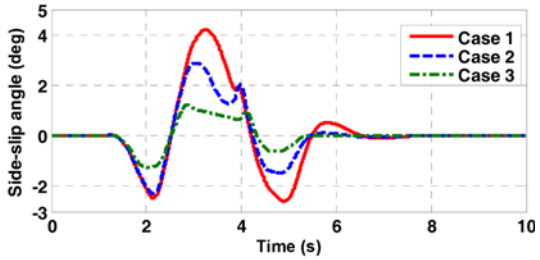

(b) Side-slip angle

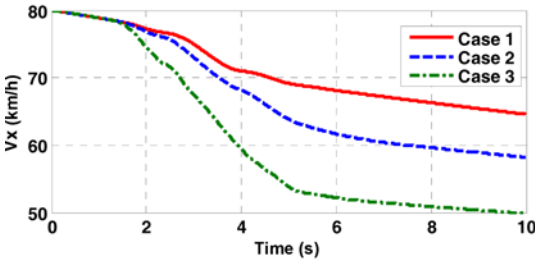

(c) Vehicle speed

Figure 5. Simulation results for each case in ZA-LMSN.

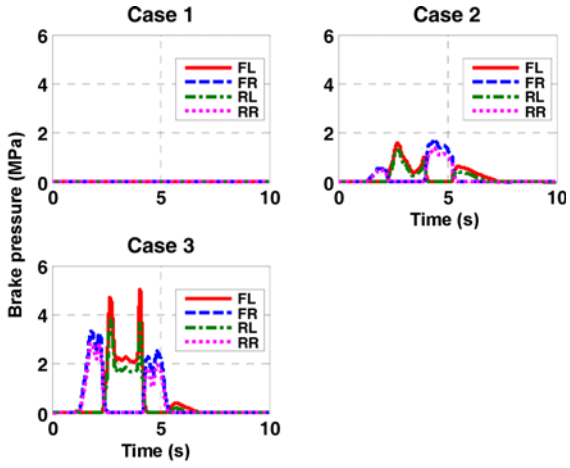

(a) Braking pressure for each case

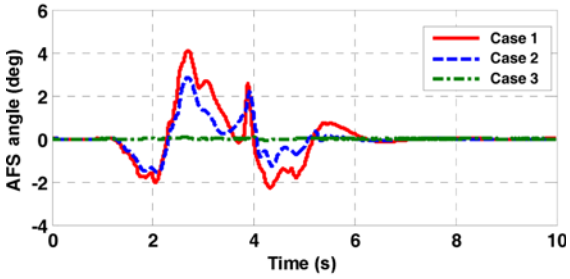

(b) AFS angle for each case

Figure 6. Control inputs for each case in ZA-LMSN.

inputs for each case in ZA-LMSN, respectively. As expected and given in Figure 6, Case 1 gave the largest side-slip angle and vehicle speed because the braking pressures were not applied. On the contrary, Case 3 did not use AFS but ESC. As a result in Figure 5, Case 3 gave the smallest side-slip angle and vehicle speed due to the largest braking input. From the results, it can be concluded that several actuator combinations in yaw moment distribution can be set by tuning the elements in the matrix **Q**. For example, Case 3 did not use AFS, and Case 1 did not use ESC. Moreover, the relative magnitude of the braking pressure of the front wheel to that of rear one can be regulated for Case 3 by setting the second and third elements differently in **Q**.

4. CONCLUSION

In this paper, the adaptive algorithms and the zero-attracting mechanism, LMS, ZA-LMS, LMSN and ZA-LMSN, were applied to yaw moment distribution in ICC. In ICC, ESC and AFS were adopted as an actuator. The WPCA was presented as a reference. To coordinate ESC with AFS, the adaptive algorithm, LMSN, was adopted. From the simulation results, it was concluded that ZA-LMSN is effective in yaw moment distribution because it is the simplest way and can regulate the relative magnitude of the control tire force of AFS to that of ESC. Moreover, it is also concluded that various responses can be obtained by setting the elements of the matrix **Q** differently in ZA-LMSN.

ACKNOWLEDGEMENT–This study was supported by the Research Program funded by the Seoul National University of Science and Technology.

REFERENCES

Chen, Y., Gu, Y. and Hero, A. O. (2009). Sparse LMS for system identification. *Proc. IEEE ICASSP*, 3125–3128.

Cho, W., Yoon, J., Kim, J., Hur, J. and Yi, K. (2008). An investigation into unified chassis control scheme for optimised vehicle stability and maneuverability. *Vehicle System Dynamics*, **46**, Supplement, 87–105.

Diniz, P. S. R. (2008). *Adaptive Filtering: Algorithms and Practical Implementation*. Springer. New York, USA.

Haykin, S. and Widrow, B. (2003). *Least-Mean-Square Adaptive Filters*. John Wiley and Sons. New Jersey, USA.

MacAdam, C. C. (1981). Application of an optimal preview control for simulation of closed-loop automobile driving. *IEEE Trans. Systems, Man, and Cybernetics* **11**, **6**, 393–399.

Mechanical Simulation Corporation (2001). CarSim User Manual Version 5.

Mokhiamar, O. and Abe, M. (2004). Simultaneous optimal distribution of lateral and longitudinal tire forces for the model following control. *ASME J. Dynamic Systems, Measurement, and Control*, **126**, 753–763.

Rajamani, R. (2006). *Vehicle Dynamics and Control*. Springer. New York, USA.

Schofield, B. (2006). *Vehicle Dynamics Control for Rollover Prevention*. Ph. D. Dissertation. Lund University. Lund, Sweden.

Shi, K. and Shi, P. (2010). Convergence analysis of sparse LMS algorithms with l_1-norm penalty basedon white input signal. *Signal Processing* **90**, **12**, 3289–3293.

Uematsu, K. and Gerdes, J. C. (2002). A comparison of several sliding surfaces for stability control. *Proc. AVEC*, Japan.

Ungoren, A. Y. and Peng, H. (2004). Evaluation of vehicle dynamic control for rollover prevention. *Int. J. Automotive Technology* **5**, **2**, 115–122.

Wang, J. and Longoria, R. G. (2006). Coordinated vehicle dynamics control with control distribution. *Proc. American Control Conf*., 5348–5353.

Wang, J., Solis, J. M. and Longoria, R. G. (2007). On the control allocation for coordinated ground vehicle dynamics control systems. *Proc. American Control Conf*., 5724–5729.

Widrow, B. and Sterns, S. D. (1985). *Adaptive Signal Processing*. Prentice-Hall. Englewood Cliffs, New Jersey, USA.

Wong, J. Y. (2001). *Theory of Ground Vehicles*. John Wiley and Sons. New Jersey, USA.

Yim, S., Choi, J. and Yi, K. (2012). Coordinated control of hybrid 4WD vehicles for enhanced maneuverability and lateral stability. *IEEE Trans. Vehicular Technology* **61**, **4**, 1946–1950.

Yim, S. (2015). Unified chassis control with electronic stability control and active front steering for under-steer prevention. *Int. J. Automotive Technology* **16**, **5**, 775–782.

Yim, S. (2016). Integrated chassis control with adaptive algorithms. *Proc. Institution of Mechanical Engineers, Part D: J. Automobile Engineering* **230**, **9**, 1264–1272.